Existence of NEU1 sialidase on mouse thymocytes whose natural substrate is CD5

Key words: CD5 / mRNA of 4 thymus-sialidases / NEU1 on thymocyte / NEU1-selective inhibitor / SM/J mouse

Shigeko Kijimoto-Ochiai[1, 2, 8, 10#], Tokuko Matsumoto-Mizuno[1, 9], Daisuke Kamimura[1'], Masaaki Murakami[1'], Miwako Kobayashi[2, 3], Ichiro Matsuoka[2, 3], Hiroshi Ochiai[4], Hideharu Ishida[5], Makoto Kiso[6], Keiko Kamimura[7], Toshiaki Koda[7, 10]

[1] Institute of Immunology/Institute for Genetic Medicine, Hokkaido University, N15W7, Sapporo 060-0815, Japan.

[1'] Institute for Genetic Medicine, Division of Molecular Psychoimmunology, Hokkaido University, N15W7, Sapporo 060-0815, Japan.

[2] Creative Research Institution (CRIS), Hokkaido University, N21 W10, Sapporo 001-0021, Japan

[3] Present address: Matsuyama Univ. College of Pharmaceutical Sciences, Bunkyo-cho, Matsuyama, Ehime 790-8578, Japan

[4] Emeritus professor of Hokkaido University, Sapporo 060-0808, Japan

[5] Faculty of Applied Biological Sciences and Center for Highly Advanced Integration of Nano and Life Sciences (G-CHAIN) Gifu University, Gifu 501-1193, Japan

[6] Organization for Research and Community development, Gifu University, Gifu 501-1193, Japan

[7] Faculty of Advanced Life Science, Hokkaido University, N21 W11, Sapporo 001-0021, Japan

[8] Present address: Life Space COSMOS (Hirosaki, 036-8222, Japan)

[9] Present address: Stadionvej 15, DK6650 Brorup, Denmark

[10] 1st Corresponding author: E-mail: sko@cris.hokudai.ac.jp or cosmosko060@me.com

Tel and Fax: +81-172-88-6636

2nd Corresponding author: E-mail: t-koda@sci.hokudai.ac.jp

Tel: +81-11-706-9062 Fax: +81-11-706-9210

[#] To whom proofs should be addressed.

Running title: NEU1 on mouse theymosytes whose natural substrate is CD5

Supplementary data: One supplementary table.

Abstract

Membrane-bound sialidases in the mouse thymus are unique and mysterious because their activity at pH 6.5 is equal to or higher than that in the acidic region. The pH curve like this has never been reported in membrane-bound form. To clarify this enzyme, we studied the sialidase activities of crude membrane fractions from immature-T, mature-T and non-T cells from C57BL/6 mice and from SM/J mice, a strain with a defect in NEU1 activity. Non-T cells from C57BL/6 mice had high activity at pH 6.5, but those from SM/J mice did not. *Neu1* and *Neu3* mRNA was shown by real-time PCR to be expressed in T cells and also in non-T cells, whereas *Neu2* was expressed mainly in non-T cells and *Neu4* was scarcely expressed. However, the in situ hybridization study on the localization of four sialidases in the thymus showed that *Neu4* was clearly expressed. We then focused on a sialidase on the thymocyte surface because the possibility of the existence of a sialidase on thymocytes was suggested by peanut agglutinin (PNA) staining after incubation of the cells alone in PBS. This activity was inhibited by NEU1-selective sialidase inhibitor C9-butyl-amide-2-deoxy-2,3-dehydro-*N*-acetylneuraminic acid. The natural substrate for the cell surface sialidase was identified as clustered differentiation 5 (CD5) by PNA-blot analysis of anti-CD5 immunoprecipitate. We conclude that NEU1 exists on the cell surface of mouse

thymocytes and CD5 is a natural substrate for it. Although this is not the main reaction of the membrane-bound thymus-sialidases, it must be important for the thymus.

Introduction

Removal of sialic acids from the cell surface of thymocytes would greatly affect cell–cell interaction, which is important in the thymus. Indeed, we found that the mouse thymus exhibited a high level of sialidase activity at neutral pH in the crude membrane fraction (Kijimoto-Ochiai et al. 2004, 2008), when compared with other organs, such as lymph nodes or the spleen, though its location on the cell surface was not proved. However, the activity of membrane-bound sialidase in the thymus is unique and mysterious because the activity level at pH 6.5–7 was nearly equal to or higher than that at acidic pH (Kijimoto-Ochiai et al. 2004, 2008, 2013). We have not found such a sialidase in membrane-bound form so far.

Four kinds of vertebrate sialidase, lysosomal NEU1, cytosolic NEU2, plasma membrane NEU3 and mitochondrial/lysosomal/intracelluar membrane NEU4, are well established and comprehensive reviews on these sialidases have been published (Monti et al. 2010; Miyagi and Yamaguchi 2012). However, many studies conducted in the past decade have shown that NEU1 is present in the plasma membrane in many cases, and NEU1 has emerged as a key

actor involved in cell signaling regulation (Pshezhetsky and Hinek 2011; Miyagi and Yamaguchi 2012; Maurice et al. 2016). NEU3, a plasma membrane sialidase, is also involved in the regulation of transmembrane signaling at the cell surface through modulation of gangliosides as the result of enzyme reactions and by interaction with other molecules. As suggested (Miyagi and Yamaguchi 2012), NEU1 and NEU3 have opposite roles in some cases such as endothelial cell migration (Cross et al. 2012), EGF receptor activation and apoptosis of human colon cancer cells. The results of a recent study suggested direct desialylation and activation of the EGF receptor by NEU3 (Mozzi et al. 2015) in addition to indirect EGFR activation through GM3. Thus, also in the thymus, NEU1 or NEU3 or both may play roles on the cell surface.

The thymus, however, is a unique organ. In a young adult mouse, the thymus contains about 10^8–2×10^8 developing T cells known as thymocytes. About 5×10^7new cells are generated each day; however, only about 10^6–2×10^6 (roughly 2–4%) of these cells leave the thymus each day as mature T cells, and about 98% of the thymocytes die by apoptosis through positive or negative selection with T cell receptor (TCR)/self-peptide:self MHC complex interaction. This apparently profligate waste of thymocytes is a crucial part of T cell development because it reflects the intensive screening that each thymocyte undergoes for the

ability to recognize self-peptide:self MHC complexes and for self-tolerance (Murphy 2012). During the development of thymocytes, they are marked by changes in many cell-surface molecules, and they interact with other cells such as cortical or medullary epithelial cells, dendritic cells and macrophages. Although there are some reports that NEU1 and NEU3 were induced differently in human T cells via T cell receptor (Wang et al. 2004) or NEU1 was expressed in plasma membrane during monocyte differentiation (Liang et al. 2006), little is known about the participation of the sialidases during these thymic immune processes. We found a unique sialidase positive cell in the mouse thymus that has IgG and Mac-1 antigens by in situ active staining using 5-bromo-4-chloro-3-indolyl-α-D-*N*-acetylnueraminic acid cyclohexyamine salt (X-NANA) (Kijimoto-Ochiai et al. 2004) and named it as "Neu-medullocyte" (Kijimoto-Ochiai et al. 2008). It was deleted in SM/J mice. The SM/J mouse is known as a sialidase-deficient $Neu1^{a}$ strain (Potier et al.1979) and later, it became clear that the low level of the activity resulted from a point mutation of the *Neu1* gene (Carrillo et al. 1997; Rottier et al. 1998). In this SM/J strain, we also found that the cytosolic soluble NEU2 activity and *Neu*2 expression was deleted or very low (Kijimoto-Ochiai et al. 2008). Thus, SM/J mice deleted in appearance not only NEU1 but also Neu2 activity. Moreover, the study on sialidases has some difficulty in general that an artificial substrate is

hydrolyzed by different degree with different sialidases: NEU2 has the highest ability, followed by NEU4 and NEU1, but NEU3 has low ability (Seyrantepe et al. 2004; Kijimoto-Ochiai et al. 2013). Thus, when the activity is assayed by using 4MU-Neu5Ac with a mixture of sailidases, it is difficult to decide which sialidase caused the results.

Historically, immature and mature thymocytes were roughly separated using peanut agglutinin (PNA) lectin (Reisner et al. 1976): PNA reacts with immature T cells but not with more sialylated mature T cells. PNA recognizes the Galβ1-3GalNAc- structure (T-antigen) but not *N*-acetyl lactosamine in N-linked oligosaccharide terminals (Lotan et al. 1975; Chacko and Appukuttan 2001), and clustered differentiation 8 (CD8) has also been reported as a PNA receptor (Wu et al. 1996).

In this study, now we survey the activity and expression of the four kinds of sialidase in mouse thymus using PNA-fractionated thymocytes and show that NEU1 exists on thymocyte using NEU1-selective sialidase inhibitor C9-butyl-amide-2-deoxy-2,3-dehydro-*N*-acetylneuraminic acid (C9-BA-DANA) (Magesh et al. 2008), which was also reported as GSC-649 (Sumida et al. 2015). We identified the natural substrate for the sialidase on thymocytes as CD5 by Western blot analysis.

Results

I. Comparison of the sialidase activities of C57BL/6 and SM/J mice using crude membranes from PNA-fractionated cells

Figure 1 shows pH curves for three fractions of the thymus from C57BL/6 and SM/J mice: T-single (PNA nonaggregated, mature T cell rich fraction), T-aggregate (PNA aggregated, immature T cell rich fraction) and non-T (residual non-T cell fraction). C57BL/6 mice showed a peak at pH 6.5 in all fractions, and the activity was particularly high in the non-T fraction. In contrast, sialidase from SM/J mice did not show a peak in the neutral region, though a small peak was observed at pH 7.0 in the T-single fraction. The peak at pH 6.5 in non-T fraction was not caused by contamination of cytosolic NEU2 because we carefully prepared the crude membrane fraction from sticky non-T material to avoid NEU2 contamination (see Materials and Methods). When we compared our results with pH curves obtained with human NEU1, NEU3 and NEU4 expressed in COS-7 cells (Seyrantepe et al. 2004) (Unfortunately we do not have pH curves for mouse sialidases.), the sialidase in T-single cells from both strains of mice seemed to be NEU4 (and/or NEU1) considering the high neutral/acidic ratio of the activity and the small peak in the neutral region. T-aggregate from SM/J mice showed relatively high activity in all of the pH range compared to that from

C57BL/6 mice and the activity decreased rapidly in the neutral region (Figure 1C). The peak around pH 5–6 was not sharp possibly because of mixture of sialidases. T-aggregate from C57BL/6 mice showed roughly the same levels of activity in acidic and neutral regions. Such activities have not been reported except our previous reports (Kijimoto-Ochiai et al. 2004, 2013).

II. Relative expression levels of the four sialidases in fractionated cells from C57BL/6 and SM/J mice, and topographic in situ detection

Next, we analyzed the expression of four silaidases in the PNA-fractionated cells of C57BL/6 mice (Figure 2A) and SM/J mice (Figure 2B) by real-time PCR. In C57BL/6 mouse (Figure 2A), *Neu1* was expressed at almost the same degree in three fractions of T-single (S), T-aggregate (A) and non-T (R), whereas *Neu3* was expressed rather less in the T-single and high in the T-aggregate as well as in the residual non-T fraction. *Neu2* (Figure 2E) was expressed mainly in non-T (R) and *Neu4* (Figure 2F) was expressed scarcely. In SM/J mouse (Figure 2B), *Neu1* and *Neu3*were highly expressed in T-aggregate fraction compared to other fractions, and *Neu1* and especially *Neu3* were expressed higher than that of C57BL/6 in all fractionated fractions (Figure 2C and D).

T-single cells consist of mature thymocytes with a small amount of double-negative (DN) T cells (Holladay et al. 1993). Mature thymocytes are located in the medulla. T-aggregate cells mainly consist of immature thymocytes and they are located in the cortex. Non-T cells consist of epithelial cells, dendritic cells and macrophages and they are located mainly in the medulla with cortical epithelial cells and some macrophages located in the cortex. Thus, we next tried to localize the position where mRNAs for the four sialidases are expressed in the thymus using in situ hybridization (Figure 3).

A thymus section stained with hematoxylin–eosin (Figure 3E) showed the cortex (C) as a deep purple-colored area and the medulla (M) as a light purple-colored area. In the Figure 3A–D stained with DIG probes *Neu1–Neu4*, respectively. Roughly three different sizes of cells can be seen: arrows 1, 2 and 3 indicate sialidase positive small, middle-sized and large cells, respectively. The expression figures of *Neu1* (Figure 3A) resembled that of *Neu3* (Figure 3C): in the area of the medulla (M), a small amount of the cells 1 and 2 was observed, whereas in the cortex (C), several of large cell 3 were observed in addition to cells 1 and 2. In the case of *Neu2* (Figure 3B) and *Neu4* (Figure 3D), the cortex and the medulla were not clearly seen. Although the mRNA expression level of *Neu4* was very low when analyzed by real-time PCR (Figure 2F), we could detect its expression in Figure 3D with the

same concentration of the DIG-labeled RNA probe as that for *Neu1* or *Neu3*, and a number of large cell 3 were observed. For *Neu2* detection, we used more condensed prove than others. In addition to the three kinds of cells in *Neu2*, we can see a lined structure around the large cell 3 (Figure 3B indicated by arrow 4). In the SM/J mouse thymus, we could not detect *Neu2* mRNA expression (Figure 3F). This is consistent with the results of our previous study in which Neu-medullocyte, NEU2 enzyme activity, and *Neu2* mRNA were not detected in the SM/J mouse thymus (Kijimoto-Ochiai et al. 2008). No hybridization signals were detected using sense probes as negative controls (Figure 3G and H).

In summary, a few mature thymocytes expressed mRNAs of *Neu1* and *Neu3* in the medulla, whereas immature T cells and cortical non-T cells expressed them more frequently in the cortex. *Neu2* and *Neu4* were probably expressed in cortical and medullary non-T cells. This is consistent with the results shown in Figure 2.

The results suggest that very few thymocytes in total thymocytes express sialidases as indicated by a comparison of the number of thymocytes stained by hematoxylin–eosin and the number of thymocytes stained by the DIG probe. Moreover, the expression of mRNA does not mean the presence of the protein on cell surface, thus, the real existence of sialidases on cell surface can be rarer than the DIG-positive cases.

III. Existence of NEU1 sialidase on the thymocyte shown using flow cytometry

Although the expression of a sialidase on cell surface of thymocytes is very rare as mentioned above, we did the following experiment expecting an existence of sialidases on thymocytes. That is, if sialidases are on the cell surface, sialic acids may be removed when thymocytes are incubated in PBS alone, and asialo-sugar chains may increase and be detected by flow cytometry using fluorescein isothiocyanate (FITC)-PNA or RCA. We might expect cis- and trans-activity of sialidase NEU1 toward glycoproteins as the case for sialidase NEU3 toward ganglioside shown by Monti et al. (2010).

Figure 4A-1 shows the curves stained with FITC-PNA, and they largely differed before and after the incubation of the cells with PBS alone (compare curves 1 and 4 (bold line)). We call this effect as “incubation effect”. Similar changes were also observed after incubation of the cells with thymus crude membrane fraction (curve 2) or soluble fraction (curves 3). These changes were apparently caused by the removal of sialic acid from sugar chains on the cells, as inferred from the behavior of the cells treated with a sialidase from *Arthrobacter ureafaciens* (curve 5). In the case of SM/J mice (Figure 4A-2), the changes were small except the left side peak. Bacterial sialidase proved able to remove sialic acids (curve 5). These results indicate that sialic acid can be removed by the bacterial sialidases; however, less

sialidase activity was present on the cell surface of thymocyte of SM/J (NEU1/NEU2 defective) mouse. The similar “incubation effect” was observed with mature T cells from A/J mouse, which did not adhere to the PNA-coated dish (Figure 4A-3, compare curves 3 and 7).

Next, we tried to determine if the NEU1-selective inhibitor C9-BA-DANA affects this “incubation effect” or not (Figure 4B). Among the curves in the presence of inhibitors (Figure 4B-2–4B-5, solid line), the line that is most similar to the control curve (Figure 4B-1, solid line that was no incubation with no inhibitor) was the line with 40 μM of C9-BA-DANA (Figure 4B-2). This means that the NEU1-selective inhibitor inhibited the sialidase reaction during the incubation of cells in PBS, whereas general sialidase inhibitor DANA inhibited scarcely (Figure 4B-4 and B-5). Therefore, it was clearly shown that NEU1 brought this incubation effect.

Next, we analyzed the expression of NEU1 on thymocytes by using flow cytometry with anti-NEU1 staining (Figure 4C). C57BL/6 thymocytes were slightly stained with anti-NEU1 (Figure 4C-1), whereas those from SM/J mouse showed no staining (Figure 4C-2). We used anti-NEU4 and also anti-NEU2 antibodies to detect the cell surface sialidase, but detected none (data not shown).

Membrane proteins from C57BL/6 and SM/J mice were solubilized and Western blot was stained with anti-NEU1 (Figure 4D). Near the marker of 45 kDa, anti-NEU1 detected two bands: lower band was observed in thymocytes and non-T cells from C57BL/6 mice (Figure 4D-1, lanes 1 and 2, indicated by arrow) but not in cells from SM/J mice (Figure 4D-1, lanes 3 and 4), whereas the upper band (indicated by arrow head) was observed not only C57BL/6 mice but also SM/J mice thymocytes (Figure 4D-1, lanes 1–3). No band was detected with the second antibody alone (Figure 4D-2). We cannot determine which is NEU1 antigen from these data.

Collectively, the results show that C57BL/6 thymocytes slightly expressed NEU1 on the cell surface, whereas SM/J cells did not. This NEU1 removed sialic acid from the glycan on thymocytes during incubation of the cells alone in PBS, because this effect was inhibited by C9-BA-DANA. As the results, PNA staining pattern changed before and after the incubation.

IV. Inhibition of sialidase activity in crude membrane fractions by C9-BA-DANA and DANA

Next, inhibition of the activity by C9-BA-DANA or DANA was investigated using crude membrane fractions from thymocytes (TM) or from residual non-T cells (RM) (Figure 5). The

obtained concentration of half inhibition IC50 (μM) values of C9-BA-DANA for TM at pH 6.5 and at pH 4.8 and for RM at pH 6.5 and at pH 4.8 were 0.74, 0.15, 0.88 and 0.53, respectively, and those of DANA were 1.16, 0.65, 1.24 and 1.33, respectively. In all cases, IC50 of DANA was slightly higher than that of C9-BA-DANA, but not as high as the previously reported 10 times higher value: the reported IC50 values for human NEU1 sialidase were 10 and 143 μM for C9-BA-DANA and DANA, respectively (Magesh et al. 2008).

V. CD5 is a natural substrate for the sialidase on the thymocyte

Next, we attempted to determine the glycoprotein substrates for the cell-surface sialidase. T-single cells were incubated in PBS alone or with the thymus soluble fraction and analyzed by Western blots (Figure 6). Two glycoprotein bands of near 66 kDa of size marker were stained more strongly by PNA (Figure 6A, lane 2, arrowheads) compared with no incubation (Figure 6A, lane 1). During the incubation of cells in PBS alone, sialic acids were removed from both these glycoproteins, suggesting that these two bands were the substrates for cell-surface sialidase. On the other hand, two new bands of near 97 kDa appeared after incubating the cells with the soluble fraction of the thymus containing the cytosol-soluble

sialidase (Figure 6A, lane 3). We would like to emphasize that the substrates for cell-surface sialidase differed from those for soluble sialidase and that the sialic acids from the substrates for soluble sialidase were not removed when the cells were incubated with PBS alone (Figure 6A, lane 2), indicating that there was no substantial release of soluble sialidase from damaged cells during incubation.

Next, we tested the hypothesis that two bands near 66 kDa represented CD5 (which has a relative molecular mass of 67,000) (Jones et al. 1986). A Western blot of the solubilized proteins from the crude membrane of the thymocyte was stained with or without anti-CD5 antibody (Figure 6B, lanes 1 and 2, respectively). Two bands were detected near the 66 kDa of size marker. Next, the thymocyte were sorted into DN, double-positive (DP), CD4- and CD8-single positive T cells using flow cytometry, and their CD5 expression was determined (Figure 6C, lanes 1–4). CD4, CD8 and DN T cells mainly expressed the lower band of CD5, whereas DP cells expressed both bands at equal proportions. CD5 was highly expressed on both CD4 and CD8 single-positive (SP) T cells. DP cells represent 85% of the total thymus T cells; therefore, two heterogeneous bands in Figure 6B is reasonable. Again, Western blots of T-single cells (mainly CD4 and CD8 mature T cells) from A/J mice were stained with anti-CD5

(Figure 6D, lane 2) and with PNA (Figure 6D, lane 3, indicated by arrowheads). An apparent single band stained with ant-CD5 seemed to correspond to two faint PNA-positive bands. Next we confirmed the CD5 molecule by an immunoprecipitation experiment with anti-CD5 (Figure 6E). The molecules that precipitated with anti-CD5 from the thymocyte-membrane proteins (Figure 6E, lane 2–4) were detected with anti-CD5 or PNA. Two bands were specifically detected by anti-CD5 antibody (indicated by arrowheads in lane 2), as was the heavy chain of the antibody (indicated by * in lane 3), and all three were stained with PNA (lane 4).

Based on the results of experiments, we conclude that the two bands detected by PNA (Figure 6A, lane 2 and Figure 6D, lane 3) and anti-CD5 (Figure 6D, lane 2) were the same molecule, namely CD5, and that this was the natural substrate for the NEU1 sialidase on thymocytes.

Discussion

We demonstrated the activity of a sialidase on the cell surface of the mouse thymocytes using flow cytometry, and we found that NEU1 caused this activity and that CD5 is the natural substrate for the cell surface sialidase.

CD5 is expressed on the 70–80% of T cell surface of various species. In the thymus, its expression in T cells by flow cytometry is low on DN T cells, increased on DP T cells and higher still on SP T cells (Azzam et al. 1998). Our Western blot data (Figure 6C) were well consistent with this result. CD5 is a monomeric cell-surface glycoprotein that possesses an extracellular region consisting of three scavenger receptor cysteine-rich (SRCR) domains in tandem, a transmembrane region and an intracytoplasmic region that is well adapted for intracellular signal transduction

(UniProt, http://www.uniprot.org/uniprot/P13379-ptm_processing). In our Western blot (Figure 6), CD5 from DP T cells showed two heterogeneous bands, whereas those from others showed mainly one band. Two heterogeneous band of CD5 probably arose because of the variable glycosylation of this molecule. The possible glycosylation sites of murine CD5 were kindly analyzed by Prof. K.F. Aoki-Kinoshita using NetNGlyc1.0 (http://www.cbs.dtu.dk/services/NetNGlyc/) and NetOGlyc4.0 (http://www.cbs.dtu.dk/services/NetOGlyc/). The results showed that the asparagine residues

at 117 and 241 were both capable of N-glycosylation, with probability scores of 0.6131 and 0.700, respectively, while eight threonine residues (138T–154T) located between the first two SRCR domains were potential O-glycosylation sites with more than 0.85 scores (summarized in Supplementary Table). PNA binds to these O-glysosylation sites if sialic acids are not in the terminal. These O- and N-glycosylation sites in CD5 were probably differently glycosylated, sialilated and made two bands by one-dimensional electrophoresis. If we analyze by two-dimensional electrophoresis, probably it shows more heterogeneous spots as we have shown with MHC class II molecule or invariant chain (Katagiri et al. 1989; Kijimoto-Ochiai et al. 1989). Recent report made clear that phosphorylation of three tyrosine residues within the cytoplasmic tail of CD5 (Y429, Y441 and Y463) regulate T cell activation and T cell survival through nonoverlapping mechanisms (Mier-Aguilar et al. 2015), and regulatory T cell development was instructed by CD5 (Henderson et al. 2015). Our result suggested that NEU1 is probably involved in this system as an important step of removing sialic acids. Thus, we should consider CD5 as a specific target molecule for sialidase on thymocyte, and distinguish the CD5 molecules with or without sialic acid (also with tyrosine residues of cytoplasmic tail) as cooperating molecule with the main pair of TCR/MHC

molecules on the cell members in the thymocyte, as well as the high or low expression levels CD5 (Klein et al. 2014).

Our results showed that *Neu1* and *Neu3* were clearly expressed in the C57BL/6 mouse thymus as can be seen in Figure 2, being consistent with the expression profile suggested by analysis of EST counts in humans (Monti et al. 2010, Fig. 7, 446 p): TPM (transcripts per million) of thymus *NEU3* are listed at third, the highest number being in the esophagus followed by bone marrow and the thymus. It is reasonable because the thymus is a highly apoptotic organ, and a major function of *NEU3* has been suggested to be apoptosis (Miyagi and Yamaguchi. 2012). Thus, the high expression level of *Neu3* in the T-aggregate fraction seems to have an important meaning for apoptosis of cells that were not selected positively or were neglected. On the other hand, TPM of thymus *NEU1* are relatively small among the listed organs because there are many organs with high expression levels such as the mammary gland and adrenal gland. ZeroTPM has been reported for thymus *NEU4*.

Nevertheless, *Neu2* or *Neu4* should not be neglected in the thymus, because the relative expression level of *Neu2* was high in the non-T fraction (Figure 2E) and both sialidases were clearly detected in in situ hybridization photographs (Figure 3B and D). The major function of *Neu4* has also been reported to be apoptosis (Miyagi and Yamaguchi 2012).

We showed in Figure 4 that NEU1 exists on thymocytes and removes sialic acid during incubation of the cells alone in PBS by using a NEU1-selective inhibitor. NEU1 is a unique sialidase compared with the others: It forms a multienzyme complex with β-galactosidase and protective protein/cathepsin A (PPCA). Because of its association with PPCA, which acts as a molecular chaperone, NEU1 is transported to the lysosomal compartment, catalytically activated and stabilized (Bonten et al. 2014). *Neu1*, a single gene on mouse chromosome 17, was determined to be located in the H-2 locus S region using SM/J mice (Figueroa et al. 1982). In humans it locates on chromosome 6P21.33, more precisely, in the major histocompatibility complex (MHC) class III region that is located between class I and class II (https://www.ncbi.nlm.nih.gov/gene/4758). This location of the *Neu1*gene must have an important meaning because MHC class II molecules in the thymus present self-antigens to T cells to remove self-reactive T cells. To contact these self-antigens, MHC class II is delivered to the so-called late endosomal MHC class II compartment (MIIC) (Garstka and Neefjes 2013) or lysosome/MIIC (Klein et al. 2014) or Endsome/MVB (ten Broeke et al. 2013) and is transferred to the cell surface. Among these processes, a part of NEU1 might move to the cell surface with MHC class II, though further study is needed to determine this.

We will now consider about the sialidase in the crude membrane fractions from T cells or non-T cells on the basis of the results shown in Figures 1, 2 and 5. Regarding the sialidase from the T cell crude membrane, higher activity observed with SM/J mice than C57BL/6 mice in T-aggregate fraction (Figure 1C) may be due to NEU1 or NEU3 considering the results shown in Figure 2C and D. NEU3, however, does not show high activity with 4MU-NANA as a substrate, whereas NEU1 activity in SM/J mouse may be low even though mRNA expression level is high because of a point mutation. In the experiment on inhibition of activity for which results are shown in Figure 5, IC50 values of C9-BA-DANA in all cases (TM, RM, acidic, neutral pH) were lower than those of DANA. Thus, it seems that at least NEU1 was involved in these fractions, but it was not the typical case of NEU1 alone: NEU1 did not show such a pH curve, and DANA cannot inhibit the NEU1 activity at such a low concentration. Next, regarding the sialidase from the non-T cell crude membrane, the activity of the non-T fraction from C57BL/6 mice was higher than that from SM/J mice and the non-T fraction showed high activity at neutral pH (Figure 1D). Among the results in the Figure 2 of non-T fraction (R), only *Neu2* (Figure 2E) showed the higher expression level of mRNA from C57BL/6 than that from SM/J mice. IC50 values of DANA for human NEU2, NEU3, NEU4 and NEU1 were 43, 61, 74 and 143, respectively (Magesh et al. 2008). Therefore, NEU2 is

inhibited by the lowest concentration of DANA among the four kinds of sialidase. We cannot deny the possibility of NEU2 in non-T crude membrane fraction from C57BL/6 mice (Figure 1D) that interacted with crude membrane fractions by an unknown mechanism. The NEU1-selective inhibition of C9-BA-DANA was explained by the steric hindrance between the inhibitor and a loop between the seventh and eighth strands of the β-propeller fold, which was substantially shorter in NEU1 than in the others (Hyun et al. 2016). This position probably corresponds to the blade II-B β-sheet and α-helices in the human cytosolic sialidase NEU2 proposed by Chavas et al. (2005). In the future, we could get some clue to explain the case of the mouse thymus sialidase if we examine the difference in the amino acid sequence between humans and mice and the corresponding second and third structures of the molecule. It should also be kept in mind that the SM/J mouse thymus showed low expression of *Neu2*, NEU2 enzyme activity, and no Neu-medullocytes (Kijimoto-Ochiai et al. 2008). Deletion of *Neu2* was also confirmed (Kijimoto-Ochiai et al. 2008) using SMXA recombinant mice (Nishimura et al. 1995).

As a future study, the enzyme of the membrane-bound thymus sialidase that shows optimal pH at 6.5 should be made clear. There are two possibilities at present: one is that mouse NEU2 is able to interact with membrane fractions because of the amino acid difference in mice and

humans, and another possibility is that mouse NEU1, NEU3 or NEU4 is able to show optimal pH at 6.5 because of the amino acid difference in mice and humans. For the first possibility, we have found by using COS cells transfected with mouse *Neu2* type B (mouse thymus-specific type, Kotani et al. 2001) that 30–40% of the activity was located in the crude membrane fraction, and hydrolyzed ganglioside mixture effectively (Koda et al. 2009). Microscopic study by active staining with X-NANA showed that the transfected gene was expressed not only in the cytoplasm but also in areas surrounding the nucleus and in the peripheral ruffled spot (Koda et al. 2009). However, further confirmation is needed: it might be important to think about the 3D structure of the sialidases based on the crystal structure of the human cytosolic sialidase NEU2 (Chavas et al. 2005) with the differences between humans and mice, e.g. hydrophobicity analysis between humans and mice of NEU2 surface molecules using an atomic-level hydrophobic scale (Kapcha and Rossky 2014). For the second possibility, we should perform a study to determine whether mouse *Neu1, Neu3* or *Neu4* gene-transfected cells show activity at pH 6.5 that is similar to or higher than that in the acidic region. In addition, the studies on new direction such as hetero dimerization (Bonten et al. 2009) or homo dimerization (Maurice et al. 2016) of NEU1 might give a clue to explain the optimal pH activity at pH 6.5 in mice. Furthermore, although high activity at pH 6.5 in the non-T fraction was remarkable (Figure 1C),

it is still unclear what cells, cortical epithelial cells, medullary epithelial cells, dendritic cells or macrophages, caused the activity. This should also be clarified.

There are still many unclear steps in addition or removal of sialic acids in the thymus. For example, many galectin-family members (soluble galactose-binding lectins) exist in the thymus and each of them has a function (Hernandez and Baum 2002; Laderach et al. 2010.). The steps in addition or removal of sialic acid in the thymus are probably related to galectin functions, for example, to prevent or expose the cells from being attacked by galectin. The siglec family (Crocker et al. 2007) may also be involved. In the future, it is necessary and important for the glycoimmunology field to uncover the many complicated unknown steps occurring in the small organ, thymus, one by one.

Materials and Methods

Mice

C57BL/6 mice and A/J mice were purchased from Japan SLC, Inc. (Hamamatsu, Shizuoka, Japan). SM/J mice were provided by RIKEN BRC (Tsukuba, Ibaraki, Japan) through the National Bio-Resource Project of the MEXT, Japan. All animal care and experimental procedures in this study were approved by Hokkaido University Animal Experiment Committee and adhered to the guidelines for animal experimentation of Hokkaido University.

Chemicals and antibodies

The following chemicals were obtained from commercial sources: Propidium iodide (Sigma), NBT/BCIP (Roche Molecular Biochemicals), sialidase from *A. ureafaciens* (Nacalai Tesque, Kyoto, Japan), rainbow size marker (Amersham, GE Healthcare, RPN756), PNA (Seikagaku Kogyo, Co. Ltd., Tokyo, Japan), PNA-biotin and FITC-PNA (J-Oil Mills, Inc. Tokyo, Japan), Vectastain Elite ABC reagent (Vector, USA), ECL Advance™ Western Blotting Detection Kit (GE Healthcare), anti-CD5 (Q-20, goat polyclonal IgG for mouse CD5 at the N-terminus, Santa Cruz Biotechnology, Inc., CA., USA), biotin-labeled donkey anti-goat IgG (G100; Santa Cruz), anti-NEU1 antibody–middle region (rabbit polyclonal antibody, ARP44286_T100, from Aviva Systems Biology), and FITC-labeled goat anti-rabbit IgG (Jackson Immuno Research Inc), DANA (Sigma). C9-BA-DANA was prepared as previously described (Megash et al. 2008).

Preparation of T cells, non-T cells and PNA-aggregated T (T-aggregate), PNA-unaggregated T cells (T-single) from thymus

From the fresh thymus, total thymocytes and the residual (non-T) cells were prepared as previously described (Kijimoto-Ochiai et al. 2013). Alternatively, they were also prepared by the treatment of enzymes (collagenase and DNase) (Gray et al. 2002). Total thymocytes were

fractionated by PNA into PNA-aggregated T cells (T-aggregate) and PNA-unaggregated T cells (T-single) (Reisner et al. 1976) by overlaying on 20% FCA as previously described (Kijimoto-Ochiai et al. 2008). Alternatively, T-single cells were obtained by PNA-coated dish method (Rothenberg 1982).

Preparation of crude membrane fraction from thymocyte, and non-T cells, solubilization and immunoprecipitation

The crude membrane fraction from the fractionated T cells was prepared and solubilized as previously described (Kijimoto-Ochiai et al. 2013). From non-T cells, we prepared the crude membrane fraction carefully to avoid the contamination of Neu2 soluble sialidase, because this fraction was very sticky and viscous with DNA. We homogenate this material in 1 mM Na_2HCO_3/0.1 mM $CaCl_2$/containing 200 μg phenylmethyl sulfonyl fluoride/mL using Dounce homogenizer by hand with 40 strokes, and then the suspension was freeze/thawed for three times to avoid the involvement of intact cells and sonicated in sonication buffer containing RNase and DNase. During these processes, the produced coagulated jell like or thread like DNA was removed. Then crude membrane fraction was separated from soluble fraction by centrifuged for 100,000 × *g* for 1 h. The precipitate was added sonication buffer,

and sonicated to suspend the crude membrane, and the protein concentration was determined and assayed for sialidase activity.

The crude membrane was solubilized as described (Kijimoto-Ochiai et al. 2004) and used for SDS-PAGE or immunoprecipitation experimant. For immunoprecipitation, the solubilized materials (30 μL per lane) were incubated with an anti-CD5 antibody (3 μg per lane) on ice for 1 h with occasional mixing, then added to Protein G Sepharose (25 μL per lane) that had been washed with TBS (50 mM Tris and 150 mM NaCl, pH 7.5). This mixture was then reacted for 1 h with rotation at 4°C. After centrifugation at 12,000 × *g* for 20 s, the supernatant was removed and the Sepharose was washed three times with 1 mL of TBS. Immunoprecipitated proteins were recovered from the washed Sepharose by heating at 95°C for 3 min in 30 μL of 2× SDS-PAGE sample buffer and subjected to SDS-PAGE.

Sialidase activity

4MU-Neu5Ac was used as a substrate and released 4MU was measured by a spectrofluorometer (molecular Device, Specta mx M5, Japan) as described in a small scale method (Kijimoto-Ochiai et al. 2013). For inhibition experiment, DANA or C9-BA-DANA

was added to the incubation mixture with appropriate concentrations described in the figures. IC50 values were calculated by means of linear regression analysis using Microsoft Excel.

A reverse transcription/polymerase chain reaction

RNA extraction and real time PCR were done essentially as described in Kijimoto-Ochiai et al (2008), except that FastStart Essential DNA Green Master mix and Light Cycler Nano system (Roche Diagnostics, Mannheim, Germany) were utilized and cDNA equivalent to 50 ng total RNA was used in each reaction. Primers for Neu1, Neu2, Neu3 and β-actin are the same as listed in the above literature. Especially, Neu2 primers can amplify all transcription variants of Neu2 (Koda et al. 2009). Primers for Neu4 were 5’-GGCAGTGTTCGAGATCTCACT-3’ and 5’-CAGCAGATCTTGCCAAAACA-3’ that can amplify both long and short forms of Neu4 (Yamaguchi et al. 2005). Total brain RNA was employed as positive control in the reaction of Neu4.

***In situ* hybridization**

To prepare probes for hybridization, cDNA fragments were amplified using the primer pairs 5’-ATGTGACCTCGACCCTGAG-3’ (forward, F) and 5′-AATCAAAGGTGCACACGTAGG -3′ (reverse, R) for Neu1, 5′-CACCCTGCTCAGAAGCCTAC -3′ (F) and 5′-TGACAACCGACATGCAGAAT -3’ (R) for

Neu2, 5’-GTGTTCAGTCAAGCCCCATT-3′ (F) and 5′- GCACATGGCCTCTCCTTTTA -3’ (R) for Neu3, 5’- GCCAGAGGTCTTCTTGAACG -3′ (F) and 5′- AACCTGCTTCTCCTGCTTGA -3′ (R) for Neu4, and 5′- GTGGGGCGCCCCAGGCACCA -3′ (F) and 5′- CTCCTTAATGTCACGCACGATTTC -3′ (R) for β-actin.

Sialidase cDNA fragments obtained from this RT-PCR were cloned into pGEM-T easy vectors (Promega, Madison, WI). Plasmid DNA was linearized using the restriction enzyme *Sal*I, except for a Neu1 plasmid that was linearized with *AccI*. Antisense RNA and sense RNA probes labelled with digoxigenin (DIG) were synthesized using T7 or Sp6 RNA polymerases (Ochiai et al. 2011). Frozen tissues were sliced by the following procedures. In brief, mouse (9-week-old) thymuses were dissected, rinsed with PBS and embedded in an OTC freezing medium (Tissue-Tek, Sakura, Finetek) and frozen in liquid N_2. Frozen thymuses were cut into 10-μm sections using a cryostat (Leica, CM 3050S) mounted on silane-coated slide glass, dried and stored at −70°C until use. These sections were processed as described (Motomiya et al. 2007) in the application manual for nonradioactive *in situ* hybridization (Roche Applied Science 3rd Ed.), with some modifications. In brief, sections were fixed in 4% paraformaldehyde and 0.5% glutaraldehyde/PBS and incubated with 1 μg/mL of proteinase K at 37°C for 10 min. After acetylation with 0.25% acetic anhydride at room temperature for 10

min, sections were dehydrated and prehybridized for 1 h at 48°C or 60°C in a prehybridization buffer containing 50% deionized formamide, 4x standard saline citrate (SSC; 15mM sodium-citrate, pH7.4, in saline), 1x Denhard's solution, 0.05% salmon sperm DNA and 0.005% tRNA. Next, sections were incubated in a hybridization buffer containing 1 μg/mL of either an antisense riboprobe or a sense probe (negative control) and 10% dextran sulfate at 48°C or 60°C overnight in a humidified box. Each slide was subjected to successive incubation in 50% formamide in 2x SSC for 30 min at 60°C after washing in 5x SSC at 60°C in 25 μg/ml of RNaseA at 37°C for 30 min and then once in 2x SSC and twice in 0.2x SSC at 60°C for 20 min each. After incubation for 60 min in a blocking reagent, immunoassay was performed using an anti-DIG–alkaline phosphatase conjugate. The color substrates NBT/BCIP were used to detect signals. The concentration of a DIG-labeled RNA probe was quantified using serial dilution with 1μg/mL of the hybridization solution, whereas a higher probe concentration was used to detect lower expression levels of Neu2 mRNA. Stained sections were washed with PBS, covered with crystal/Mount^{TM} (Biomeda Corp., Foster City, CA.) and were dried on a heater.

Flow cytometry

For detection of the sialidase activity (Fig. 4), the total thymocyte or T-single were incubated

with the crude thymus membrane fraction, the soluble fraction from a frozen thymus (which was expected to have endogenous sialidase), sialidase from *A. ureafaciens* or PBS (mock incubation) in 60 μL of isotonic solution (30 μL of cell suspension plus 30 μL of sialidase in isotonic solution). After incubation at 37°C for 30–60 min with or without inhibitor, the cells were washed and incubated with FITC-PNA 0.1% bovine serum albumin–0.1% sodium azide in PBS (flow cytometry buffer) on ice for 30 min. For the detection of the sialidase on thymocyte by antibody (Fig. 4C), the thymocytes were incubated with anti-NEU1, for 1 h on ice, washed, and then with FITC-labeled second antibody (goat anti-rabbit IgG). The cells were washed twice with PBS, suspended in flow cytometry buffer, and passed through a nylon mesh. Propidium iodide (5 ng) was added to the cells immediately before data acquisition to electronically exclude non-viable cells. The data in Fig. 4 were obtained with a CyAn flow cytometer (Beckman Coulter) using the FlowJo software (FlowJo, LLC) except the data in Fig. 4A-3 which was obtained with a FACScan flow cytometer (Becton Dickinson Co., Mountain View, CA, USA) using the AutoCOMP software (Becton Dickinson) and the acquired events (about 30,000) were analyzed using the Cell Quest software (Becton Dickinson).

T cell sorting into DN, DP, CD4- and CD8-SP T cells

This was done according to our previous report (Kijimoto-Ochiai et al. 2013).

Detection of Natural substrate for Sialidase on thymocyte

Thymus cells were prepared from two A/J 7-week-old mice and incubated in two PNA-coated plates (10-cm diameter) at 22°C for 90 min, as described above. Non-adherent (T-single) cells were harvested, washed, and a cell suspension was aliquoted into three small tubes. The cells in the first tube were centrifuged and frozen immediately, the cells in the second and third tube were incubated in PBS or in a soluble fraction at 37°C for 60 min in a CO_2 incubator, respectively, and were then washed and frozen. From the frozen cells of the three tubes, a crude membrane fraction was obtained and solubilized with detergent as previously described (Kijimoto-Ochiai et al. 2008), subjected to SDS-PAGE, and the Western blot was stained with PNA or anti-CD5 as follows.

SDS-PAGE and Western blot analysis

These were performed under reducing conditions as previously reported (Kijimoto-Ochiai et al. 2013), using a rainbow size marker. The western blots were blocked with 2% blocking reagent (GE Healthcare) and then treated in one of three ways: (1) reacted with biotin-labeled PNA, followed by Vectastain Elite ABC reagent containing avidin-peroxidase (Vector, USA); (2) reacted with anti-CD5 and then biotin-labeled donkey-anti-goat IgG, followed by

Vectastain Elite ABC reagent containing avidin–peroxidase; or (3) reacted with anti-NEU1 antibody and then HRP-linked donkey anti-rabbit IgG. In all three cases, the blots were reacted using an ECL Advance™ Western Blotting Detection Kit (GE Healthcare) and enhanced chemiluminescent signals were detected with a Molecular Imager (BioRad).

Acknowledgements

The authors would like to thank Prof. K.F. Aoki-Kinosita (Soka University, Japan) who introduced us to the glycosylation prediction software and analyzed the murine CD5 glycosylation. We thank Prof. emerita K. Moriya (Hokkaido University) for introducing us to Ms. T. Matsumoto-Mizuno who performed flow cytometry analysis at the Institute of Immunology, Ms. A. Shibanuma for technical assistance in the maintenance of mice, Dr. Hino and Prof. S. Nishimura for spectrofluorometer in Post Genome Center, Dr. S. Mitsutake, Dr. Yuyama and Prof. Y. Igarashi for the ultracentrifuge and sonicator in the Faculty of Advanced Life Science at Hokkaido University and Shionogi Innovation Center for Drug Discovery, Dr. K. Azumi for the space to continue in situ hybridization research after Prof. I. Matsuoka moved to Matsuyama University, and the Open Facility (Hokkaido University Sousei Hall) for the cryostat (Leica, CM 3050S) and for the Molecular Imager ChemiDoc™ (BioRad). This research did not receive any specific grant from funding agencies in the public,

commercial, or not-for-profit sectors.

Funding

This research did not receive any specific grant from funding agencies in the public, commercial or not-for-profit sectors.

Conflict of interest statement

None declared.

Abbreviations: *A*, *Arthrobacter*; CD, clustered differentiation; DN, (CD4/CD8) double-negative; DP, double-positive; SP, single-positive; FCS, fetal calf serum; FITC, fluorescein isothiocyanate; PMSF, phenylmethyl sulfonyl fluoride; 4MU-Neu5Ac, 4-Methylumbelliferyl 5-acetyl neuraminic acid; PNA, peanut agglutinin; NBT/BCIP, nitro blue tetrazolium/ 5-bromo-4-chloro-3-indoly phosphate; DIG, digoxigenin; DANA, 2-deoxy-2,3-dehydro-N-acetylneuraminic acid; C9-BA-DANA, C9-butyl-amide-2-deoxy-2,3-dehydro-N-acetylneuraminic acid.

References

Azzam HS, Grinberg A, Lui K, Shen H, Shores EW, Love PE. 1998. CD5 expression is developmentally regulated by T cell receptor (TCR) signals and TCR avidity. *J Exp Med.*

188:2301-2311.

Bonten EJ, Annunziata I, d'Azzo A. 2014. Lysosomal multienzyme complex: Pros and Cons of working together. *Cell Mol Life Sci.* 71: 2017-2032.

Bonten EJ, Campos Y, Zaitsev V, Nourse A, Waddell B, Lewis W, Taylor G, d'Azzo A. 2009. Heterodimerization of the Sialidase NEU1 with the Chaperone Protective Protein/Cathepsin A Prevents Its Premature Oligomerization. *J Biol Chem*. 284:28430-28441.

Broeke Tt, Wubbolts R, Stoorvogel W. 2013. MHC class II antigen presentation by dendritic cells regulated through endosomal sorting. Cold Spring Harb Perspect Biol. 5:a016873.

Carrillo MB, Milner CM, Ball ST, Snoek M, Campbell RD. 1997. Cloning and characterization of a sialidase from the murine histocompatibility-2 complex: low levels of mRNA and a single amino acid mutation are responsible for reduced sialidase activity in mice carrying the $Neu1^a$ allele. *Glycobiology.* 7:975-986.

Chacko BK, Appukuttan PS. 2001. Peanut (*Arachis hypogaea*) lectin recognizes α-linked galactose, but not N-acetyl lactosamine in N-linked oligosaccharide terminals. *International J Biological Macromolecules.* 28:365-371.

Chavas LMG, Tringali C, Fusi P, Venerando B, Tettamanti G, Kato R, Monti E, Wakatsuki S. 2005. Crystal Structure of the human cytosolic sailidase Neu2. EVIDENCE FOR THE

DYNAMIC NATURE OF SUBSTRATE RECOGNITION. *J Bio Chem.* 280:469-475.

Crocker PR, Pau;spm JC, Varki A. 2007. Siglecs and their roles in the immune system. *Nat Rev Immunol*. 7:255-56.

Cross AS, Hyun SW, Ribera AM, Feng C, Liu A, Nguyen C, Zhang L, Kuzina IG, Atamas SP, Twaddell WS et al. 2012. NEU1 and NEU3 Sialidase Activity Expressed in Human Lung Microvascular Endothelia. NEU1 RESTRAINS ENDOTHELIAL CELL MIGRATION, WHEREAS NEU3 DOES NOT. *J Biol Chem.* 287:15966-15980.

Figueroa F, Klein D, Tewarson S, Klein J. 1982. Evidence for placing the Neu-1 locus within the mouse H-2 complex. *J Immunol*. 129:2089-2093.

Garstka MA and Neefjes J. 2013. How to target MHC classII into the MIIC compartment. *Molecular Immunology*. 55:162-165.

Gray DHD, Chidgey AP, Boyd RL. 2002. Analysis of thymic stromal cell populations using flow sytometry. *J Immunolo Methods*. 260:15-18.

Hernandez JD, Baum LG. 2002. Ah, sweet mystery of death! Galectins and control of cell fate. *Glycobiology*. 12:127R-36R.

Henderson JG, Opejin A, Jones A, Gross C, Hawiger D. 2015. CD5 instructs extrathymic regulatory T cell development in response to self and tolerizing antigens. *Immunity*.

42:471-483

Holladay S, Blaylock B, Smith B, Luster M. 1993. PNA lectin-based separation of thymocytes into mature and immature subpopulations: CD4-8-double negative cells display characteristics of PNAlo mature thymocytes. *Immunol Invest.* 22:517-529.

Hyun SW, Liu A, Liu Z, Cross AS, Verceles A, Magesh S, Kommagalla Y, Kona C, Ando H, Luzina IG et al. 2016. The NEU1-selective sialidase inhibitor, C9-butyl-amide-DANA, blocks sialidase activity and NEU1-mediated bioactivities in human lung in vitro and murine lung in vivo. *Glycobiology*. 26:834-849.

Kapcha L, Rossky PJ. 2014. A simple atomic-level hydrophobicity scale reveals protein interfacial sturucture. *J Mol Biol.* 426: 484-498.

Katagiri YU, Kijimoto-Ochiai S, Hatae T, Okuyama H. 1989. Type analysis of oligosaccharide chains on human and murine MHC class II alpha chains by the lectin-nitrocellulose sheet method. *Comp Biochem Physiol*. B 93:259-263.

Kijimoto-Ochiai S, Doi N, Fujii M, Go S, Kabayama K, Moriya S, Miyagi T, Koda T. 2013. Possible association of Neu2 with plasma membrane fraction from mouse thymus exhibited sialidase activity with fetuin at pH 7.0 but not at pH 4.5. *Microbiol Immunol.* 57:569-582.

Kijimoto-Ochiai S, Doi N, Matsukawa H, Fujii M, Tomobe K. 2004. Localization of

sialidase-positive cells expressing Mac-1 and immunoglobulin in the mouse thymus. *Glycoconj J*. 20:375-384.

Kijimoto-Ochiai S, Hatae T, Katagiri YU, Okuyama H. 1989. Microheterogeneity and oligosaccharide chains on the beta chains of HLA-DR, human major histocompatibility complex class II antigen, analyzed by the lectin-nitrocellulose sheet method. *J Biochem*. 106:771-777.

Kijimoto-Ochiai S, Koda T, Suwama T, Matsukawa H, Fujii M, Tomobe K, Nishimura M. 2008. Low expression of Neu2 sialidase in the thymus of SM/J mice-existence of neuraminidase positive cells "Neu-medullocyte" in the murine thymus. *Glycoconj J*. 25:787-796.

Klein L, Kyewski B, Allen PM, Hoqquist KA. 2014. Positive and negative selection of the T cell repertoire: what thymocytes see and don't see. *Nat Rev Immunolo.* 14:377-391.

Koda T, Kijimoto-Ochiai S, Uemura S, Inokuchi J. 2009. Specific expression of Neu2 type B in mouse thymus and the existence of a membrane-bound form in COS cells. *Biochem Biophys Res Commun*. 387:729-735.

Kotani K, Kuroiwa A, Saito T, Matsuda Y, Koda T, Kijimoto-Ochiai S. 2001. Cloning, chromosomal mapping, and characteristic 5'-UTR sequence of murine cytosolic sialidase.

Biochem Biophys Res Commun. 286:250-258.

Laderach DJ, Compagno D, Toscano MA, Croci DO, Dergan-Dylon S, Salatino M, Rabinovich GA. 2010. Dissecting the signal transduction pathways triggered by galectin-glycan ineraction in physioogical and pathological settings. *IUBMB Life.* 62: 1-13.

Liang F, Seyrantepe V, Landry K, Ahmad R, Ahmad A, Stamatos NM, Pshezhetsky AV. 2006. Monocyte differentiation up-regulates the expression of the lysosomal sialidase, Neu1, and triggers its targeting to the plasma membrane via major histocompatibility complex class II-positive compartments. *J Biol Chem*. 281:27526-27538.

Lotan R, Skutelsky E, Sharon N. 1975. The purification, composition, and specificity of the anti-T lectin from Peanut (*Arachis hypogaea*). *J Biol Chem*. 250:8518 -8523.

Lukong KE, Seyrantepe V, Landry K, Trudel S, Ahmad A, Gahl WA, Lefrancois S, Morales CR, Pshezhetsky AV. 2001. Intracellular distribution of lysosomal sialidase is controlled by the internalization signal in its cytoplasmic tail. *J Biol Chem*. 276:46172-81.

Magesh S, Moriya S, Suzuki T, Miyagi T, Ishida H, Kiso M. 2008. Design, synthesis, and biological evaluation of human sialidaase inhibitors. Part 1: Selective inhibitors of lysosomal sialidase (NEU1). *Bioorg Med Chem Lett.* 18:532-537.

Maurice P, Baud S, Biocharova OV, Bocharov V, Kunnetsov AS, Kawecki C, Bocquet 0,

Romiter B, Gorisse L, Ghirardi M et al. 2016. New insights into molecular organization of human neuraminidase-1: Transmembrane topology and dimerization ability. *Sci Rep*. 6:38363.

Mier-Aguilar CA, Vega-Baray B, Burgueno-Bucio E, Lozano F, Garcia-Zepeda EA, Raman C, Soldevila G. 2015. Functional requirement of tyrosine residue 429 within CD5 cytoplasmic domain for regulation of T cell activation and survival. *Biochem Biophys Res Comm*. 466:381-387.

Miyagi T and Yamaguchi K. 2012. Mammalian sialidases: Physiological and pathological roles in cellular functions. *Glycobiology.* 22: 880-896.

Monti E, Bonten E, D'Azzo A, Bresciani R, Venerando B, Borsani G, Schauer R, Tettamanti G. 2010. Sialidases in vertebrates: a family of enzymes tailored for several cell functions. *Adv Carbohydr Chem Biochem*. 64:403-479.

Motomiya M, Kobayashi M, Iwasaki N, Minami A, Matsuoka I. 2007. Activity-dependent regulation of BRINP family genes. *Biochem Biophys Res Comm.* 352:623-629.

Mozzi A, Forcella M, Riva A, Difrancesco C, Molinari F, Martin V, Papini N, Bernasconi B, Nonnis S, Tedeschi G et al. 2015. NEU3 activity enhances EGFR activation without affecting EGFR expression and acts on its sialylation levels. *Glycobiology.* 25:855-868.

Murphy K. 2012. Janeway' s ImmunoBiology. 8th ed. London & NY: Garland Science.

Nishimura M, Hirayama N, Serikawa T, Kanehira K, Matushima Y, Katoh H, Wakama S, Kojima A, Hiai H. 1995. The SMXA: a new set of recombinant inbred strain of mice consisting of 26 substrains and their genetic profile. *Mamm Genome*. 6:850-857.

Ochiai H, Takeda K, Fukuzawa M, Kato A, Takiya S, Ohmachi T. 2011. Protein Kinase B Gene Homologue *pkbR1* performs one of Its Roles at First Finger Stage of *Dictyostelium. Eukaryotic cell*. 10:512-520.

Potier M, Shun Yan DL, Womack JE. 1979. Neuraminidase deficiency in the mouse. *FEBS Letters.* 103:345-348.

Pshezhetsky AV, Hinek A. 2011. Where catabolism meets signalling: neuraminidase 1 as a modulator of cell receptors. *Glycoconj. J.* 28:441-452.

Reisner Y, Linker-Israeli M, Sharon N. 1976. Separation of mouse thymocytes into two subpopulations by the use of peanut agglutinin. *Cell Immunol.* 25:129-134.

Rothenberg E. 1982. A specific biosynthetic marker for immature thymic lymphoblasts. Active synthesis of thymus-leukemia antigen restricted to proliferating cells. *J Exp Med.* 155:140-154.

Rottier RJ, Bonten E, d'Azzo A. 1998. A point mutation in the neu-1 locus causes the neuraminidase defect in the SM/J mouse. *Hum Mol Genet.* 7:313-321.

Seyrantepe V, Landry K, Trudel S, Hassan JA, Morales CR, Pshezhetsky AV. 2004. Neu4, a Novel Human Lysosomal Lumen Sialidase, Confers Normal Phenotype to Sialidosis and Galactosialidosis Cells. *J Biol Chem*. 279:37021-37029.

Sumida M, Hane M, Yabe U, Shimoda Y, Pearce OMT, Kiso M, Miyagi T, Sawada M, Varki A, Kitajima K et al. 2015. Rapid Trimming of cell surface polysialic acid (PolySia) by exovesicular sialidase triggers release of preexisting surface neurotrophin. *J Biol Chem.* 290:13202-13214.

Wang P, Zhang J, Bian H, Wu P, Kuvelkar R, Kung T, Crawley Y, Egan RW, Billah MM. 2004. Induction and plasma membrane-bound sialidases in human T-cells via T-cell receptor. *Biochem J.* 380:425-433.

Wu W, Harley PH, Punt JA, Sharrow SO, Kearse KP. 1996. Identification of CD8 as a peanut agglutinin (PNA) receptor molecule on immature thymocytes. *J Exp Med.* 184:759-764.

Yamaguchi K, Hata K, Koseki K, Shiozaki K, Akita H, Wada T, Moriya S, Miyagi T. 2005. Evidence for mitochondrial localization of a novel human sialidase (NEU4). *Biochem J.* 390:85-93.

Legends to figures

Fig. 1 pH curves for sialidase of the thymus from C57BL/6 and SM/J mice

Activity was assayed with 4MU-NANA and the crude membrane from T-single, T-aggregate and non-T cells using citrate-phosphate buffer (●, solid line from pH 4.0 - pH 6.0) or PIPES buffer (△, dotted line from pH 6.0 - pH 7.5). **A** and **B**: crude membrane fractions from T-single cells from C57BL/6 (B6) and SM/J mice, respectively. **C** and **D**: crude membrane fractions from T-aggregate cells and non-T cells, respectively.

Fig. 2 Relative expression levels of four sialidases in fractionated cells from C57BL/6 and SM/J mice

RNA extraction and real time PCR were done as described in Materials and Methods. **A**: relative expression levels of Neu1 and Neu3 in total thymocyte (T, white bar), T-single cell fraction (S, diagonal lined bar), T-aggregated cell fraction (A, vertical lined bar) and residual non-T fraction (R, black bar) from C57BL/6 mice compared to the expression levels of β-actin. **B**: same as **A** except SM/J mice were used. **C**, **D, E and F**: relative expression levels of *Neu1*, *Neu3*, *Neu2 and Neu4* of C57BL/6 (B6, black bar) and SM/J mice (white bar) in four fractionated cell fractions. Total brain RNA was employed as positive control in the reaction of Neu4 (Brain). All values were the average of duplicate.

Fig. 3 Localization of mRNAs for four sialidases by *in situ* hybridization

Frozen sections from A/J thymuses (7-week-old) (except **F**) and SM/J thymus (**F**) were prepared at 10-μm-thicknesses, and these sections were reacted with DIG-labeled RNA probes and stained with NBT/BCIP as described in the Materials and Method. DIG-labeled anti-sense RNA probes were used to detect *Neu1* (**A**), *Neu2* (**B**), *Neu3* (**C**), and *Neu4* (**D**). The section from the SM/J mouse thymus was stained with a *Neu2* anti-sense probe (**F**). The sense probes were used to confirm no expression *Neu1* (**G**) and *Neu2* (**H**). Photomicrograph **E**: Hematoxylin and eosin staining of a 10-μm thick A/J thymus section, in which (**C**) and (**M**) indicate the cortex and medulla areas, respectively. Photographs were acquired with a 10x objective and a 10x ocular; bar shows 1 μm. Arrows 1, 2 and 3 indicate small, middle and large DIG-positive cells. Arrow 4 in **B** indicates a lined structure.

Fig. 4 Detection of sialidase on mouse thymocytes

A. Flow cytometric analysis of the thymus cells with FITC-PNA after incubation with sialidases or PBS alone. **A-1**: Thymocytes from a C57BL/6 mouse (7 weeks old, one male) were stained with FITC-PNA on ice for 30 min after keeping on ice with no sialidase (curve 1), or after the incubation with the crude thymus membrane fraction (2, dotted line), the soluble thymus fraction (3, broken line), sialidase from *A. ureafaciens* (5), or PBS alone (4,

bold line), at 37°C for 30 min. **A-2**: Same procedure as **A-1**, except that an SM/J mouse (5 weeks old, one male) was used. **A-3**: FITC-PNA staining histogram of fractionated thymocytes from a 7-week-old A/J male mouse. T-single cells were obtained using a PNA-coated plate method as described in Materials & Methods. Cells were incubated with or without sialidases materials at 37°C for 1 h, washed and stained with FITC-PNA on ice for 30 min, washed and then analyzed by flow cytometry. Curve 1, unfractionated thymocyte, unstained; 2, unfractionated thymocyte stained with FITC-PNA; 3, T-single cells stained with FITC-PNA; 4-7, T-single cells incubated with a thymus crude membrane fraction (4), with a thymus soluble fraction (5), with a sialidase from *A. ureafacience* (6) or with PBS alone (7). **B.** NEU1-selective inhibitor C9-B-DANA inhibited the "incubation effect" on flow cytometry. The horizontal axis in B is <FL 1 Log>: FITC-PNA. **B-1**: the thymocytes from C57BL/6 mouse was kept on ice for 1h (solid line) or incubated in PBS at 37°C for 1h (bold line) and stained with FITC-PNA. **B-2, -3, -4, -5**: bold line is the same as that in B-1. Solid lines in B-2~B-5 are for incubation in the presence of 40 μM or 8 μM of C9-BA-DANA or in the presence of 200 μM or 40 μM of DANA at 37°C for 1h, respectively. **C**. Flow cytometric analysis of NEU1 antigen with anti-NEU1 antibody on the thymocyte. **C-1**: Thymocytes from C57BL/6 (5-week-old) were stained with anti-NEU1 antibody and FITC labeled 2^{nd} antibody.

The cells were incubated with anti-NEU1 (shadowed), or without antibody (dotted line). **C-2**: SM/J mice (5-week-old) were used instead of C57BL/6 mice in C-1. **D.** Blots of the solubilized membrane protein from C57BL/6 and SM/J mice were stained with anti-NEU1 (**D-1**), or with 2nd antibody alone (**D-2**). Lane 1: thymocytes and lane 2: non-T from C57BL/6 mice, and lane 3: thymocytes and lane 4: non-T from SM/J mice. The vertical axis of all flow ctyotometric data in Fig.4 except Fig. 4A-3 indicates % of maximam, whereas that in A-3 indicates cell number. The horizontal axis in A and B indicates the fluorescent intensity of FITC-PNA, and C indicates the fluorescent intensity of anti-NEU1 / FITC-2nd antibody.

Fig. 5 Inhibition of sialidase activities in thymus membrane fractions by DANA and a NEU1-seletive inhibitor C9-BA-DANA

Assays were performed using 4MUNeuAc as a substrate. The enzyme preparation was incubated for 60 min without or with inhibitors at 0.12, 1.2, 12, and 120□μM. A and B: With the thymocyte membrane fraction (TM) at pH 6.5 and at pH 4.8, activity was assayed in two series: one was at 1.2, 12, 120 and 1200 (not shown) μM of DANA (■ with dotted line) or C9-BA-DANA (○ with solid line, indicated C9-B), and the other was at 0, 0.12, 1.2 and 12 μM of inhibitors with duplicate and average values being plotted. C and D: same as A and B except the residual membrane fraction (epithelial cell rich, RM) was used.

Fig. 6 CD5 is a natural substrate for the sialidase on the thymocyte

A. PNA staining of the blot prepared from A/J mice T-single cells as described in Materials and Methods. T-single cells were no incubated (lane 1), incubated with PBS alone (lane 2) or with a soluble fraction at 37°C for 60 min (lane 3). Arrowheads indicate the bands stained more strongly with PNA after incubation. **B.** Detection of CD5 antigen. The blot of the solubilized proteins of the crude membrane fractions from the thymocytes (unfractionated with PNA) of 7-week-old A/J mice was stained with (lane 1) or without (lane 2) anti-CD5 and then its secondary antibody. **C.** CD5 molecules from sorted thymus cells. Thymocytes from two A/J mice (7-week-old) were sorted by flow cytometry into DN, DP, CD4 and CD8 T cells (lanes 1–4, respectively). The solubilized proteins from the crude membrane corresponding to 5×10^5 cells were subjected to western blotting and stained with an anti-CD5 system. **D.** Correspondence of CD5 antigen and PNA-positive bands. The western blotted antigens were as follows: lane 1, solubilized proteins from crude membrane fractions of COS cells as a CD5-negative control; lanes 2–4, T-single cells from A/J thymus cells. Each lane was stained with anti-CD5 and secondary antibody (lanes 1 and 2), secondary antibody alone (lane 4), or PNA (lane 3). **E.** Detection of anti-CD5 immunoprecipitates by anti-CD5 or PNA. The solubilized proteins from crude membrane fractions of A/J thymocyte before

immunoprecipitation (lane 1) and after immunoprecipitation (lanes 2–4) were detected with anti-CD5 and secondary antibody (lanes 1 and 2), secondary antibody alone (lane 3), or PNA (lane 4). The amount of solubilized protein used for immunoprecipitation (for each lane) was twice that used for lane 1. The heavy chain of anti-CD5 detected by the secondary antibody is indicated by *.

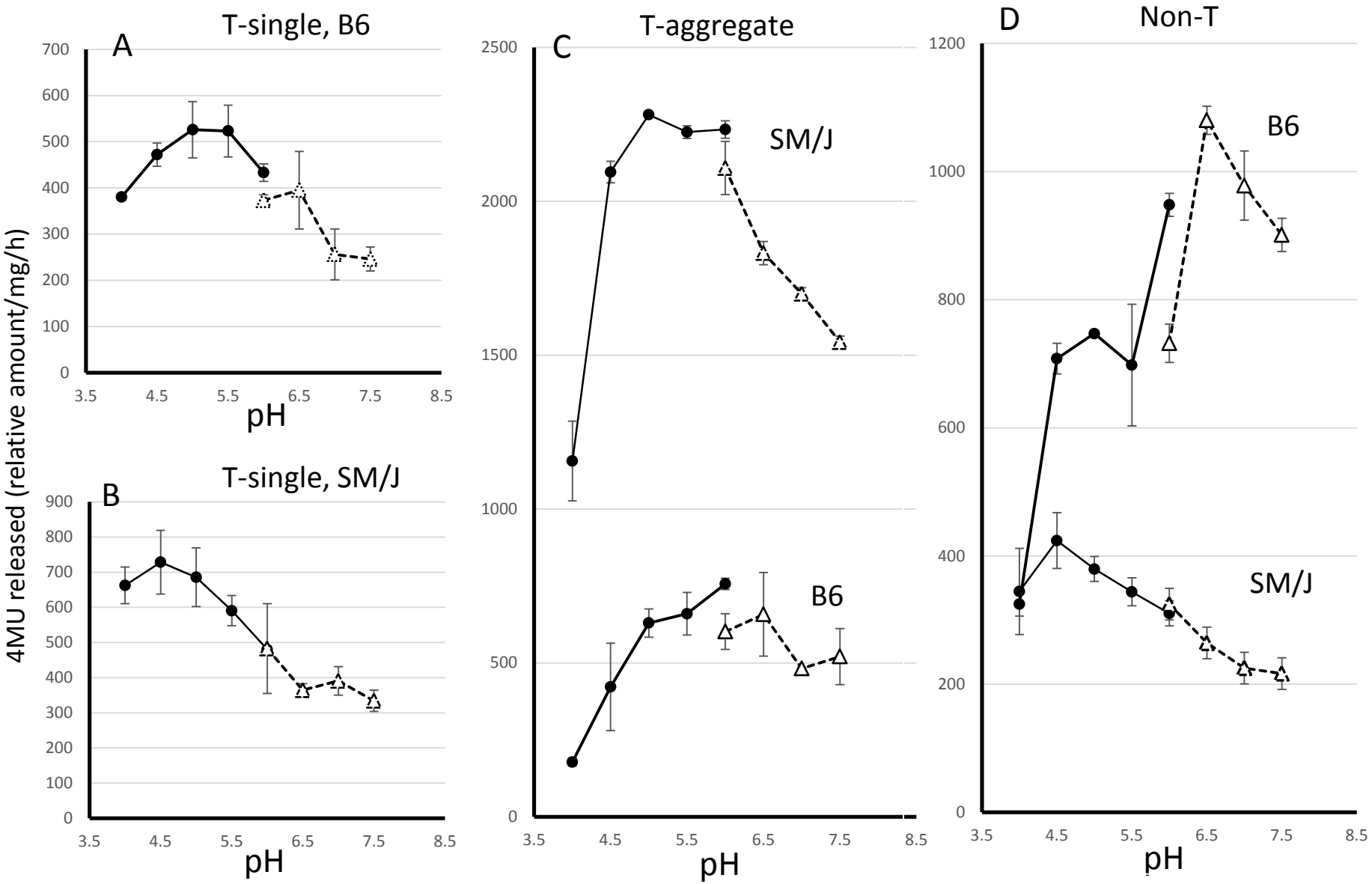
A
T-single, B6
B
T-single, SM/J
C
T-aggregate
SM/J
B6
D
Non-T
B6
SM/J
4MU released (relative amount/mg/h)
pH
pH
pH
pH

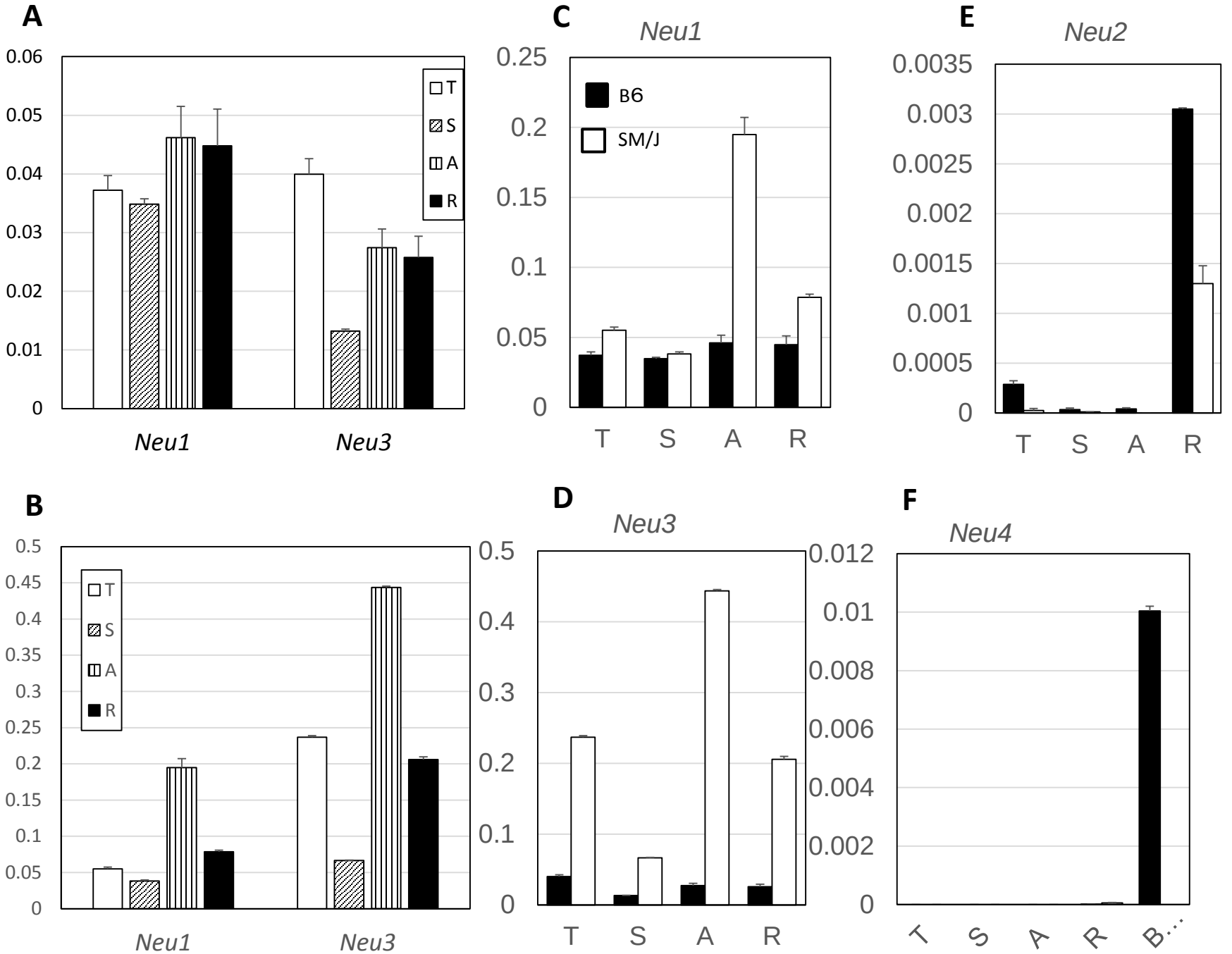
A
0.06
0.05
0.04
0.03
0.02
0.01
0
T
S
A
R
Neu1
Neu3
C
Neu1
0.25
0.2
0.15
0.1
0.05
0
B6
SM/J
T
S
A
R
E
Neu2
0.0035
0.003
0.0025
0.002
0.0015
0.001
0.0005
0
T
S
A
R
B
0.5
0.45
0.4
0.35
0.3
0.25
0.2
0.15
0.1
0.05
0
T
S
A
R
Neu1
Neu3
D
Neu3
0.5
0.4
0.3
0.2
0.1
0
T
S
A
R
F
Neu4
0.012
0.01
0.008
0.006
0.004
0.002
0
T
S
A
R
B…

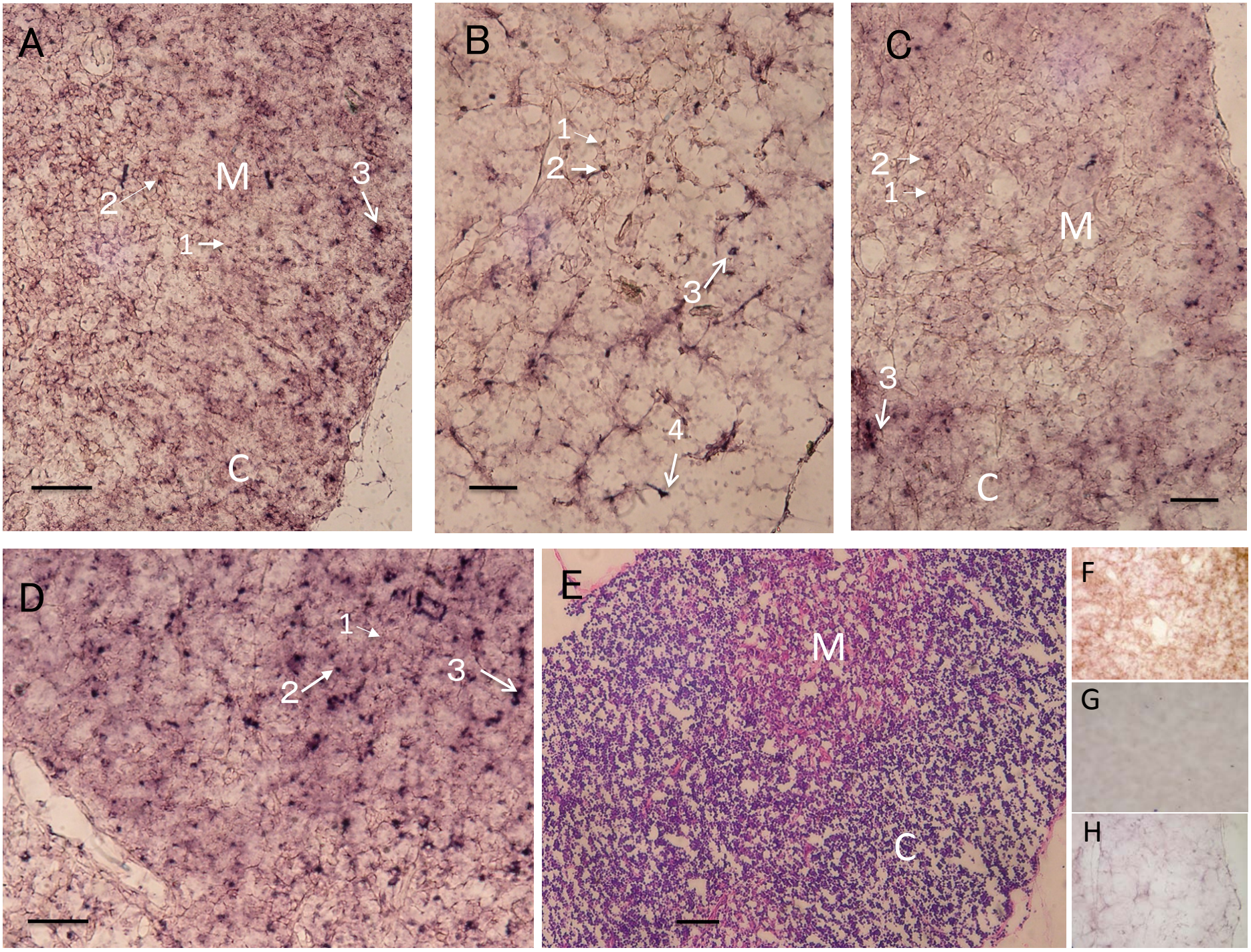
A
M
C
1
2
3
B
1
2
3
4
C
M
C
1
2
3
D
1
2
3
E
M
C
F
G
H

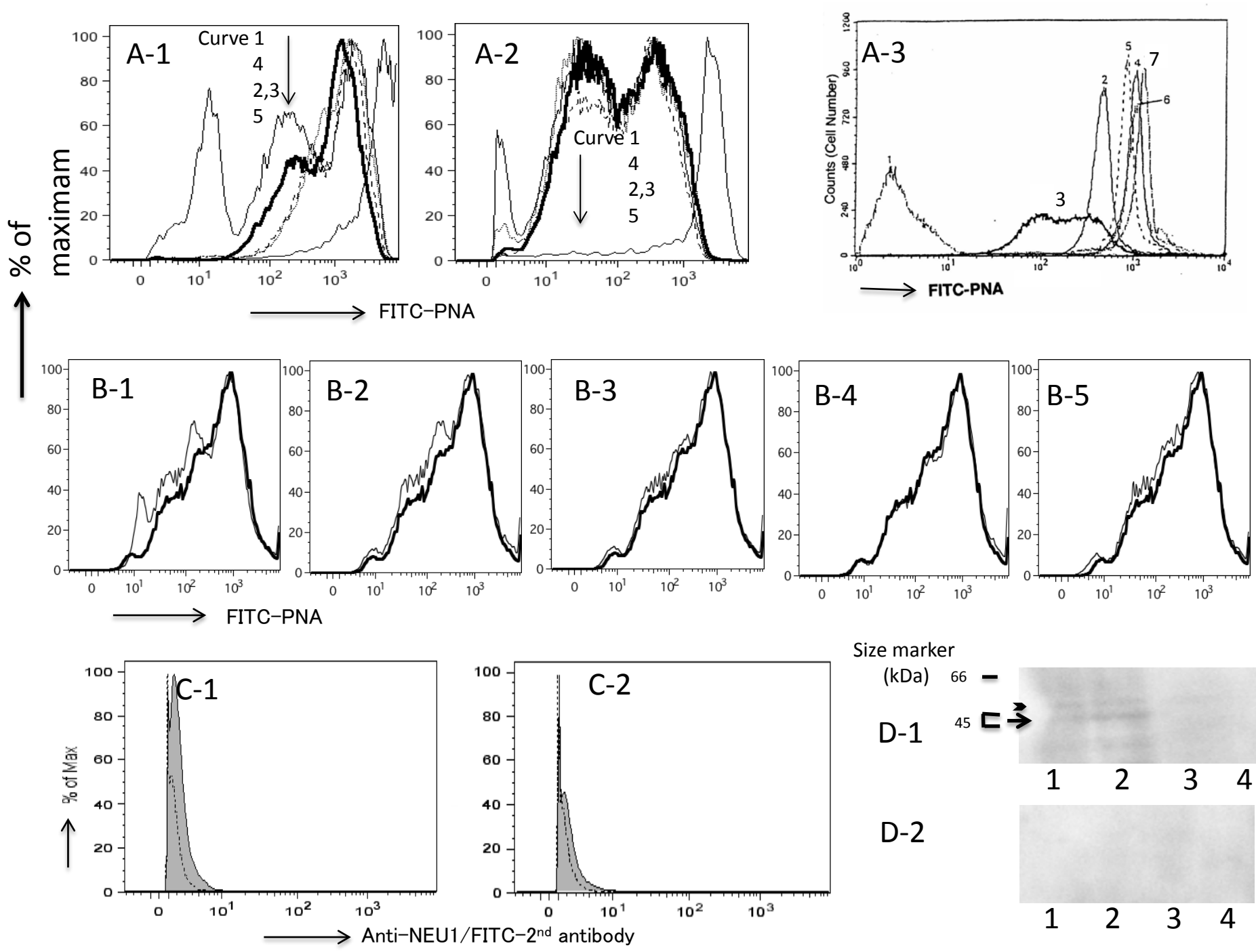
A-1
Curve 1
4
2,3
5
A-2
Curve 1
4
2,3
5
A-3
Counts (Cell Number)
FITC-PNA
% of maximam
FITC−PNA
B-1
B-2
B-3
B-4
B-5
FITC−PNA
C-1
C-2
% of Max
Anti−NEU1/FITC−2nd antibody
Size marker
(kDa)
66
45
D-1
1 2 3 4
D-2
1 2 3 4

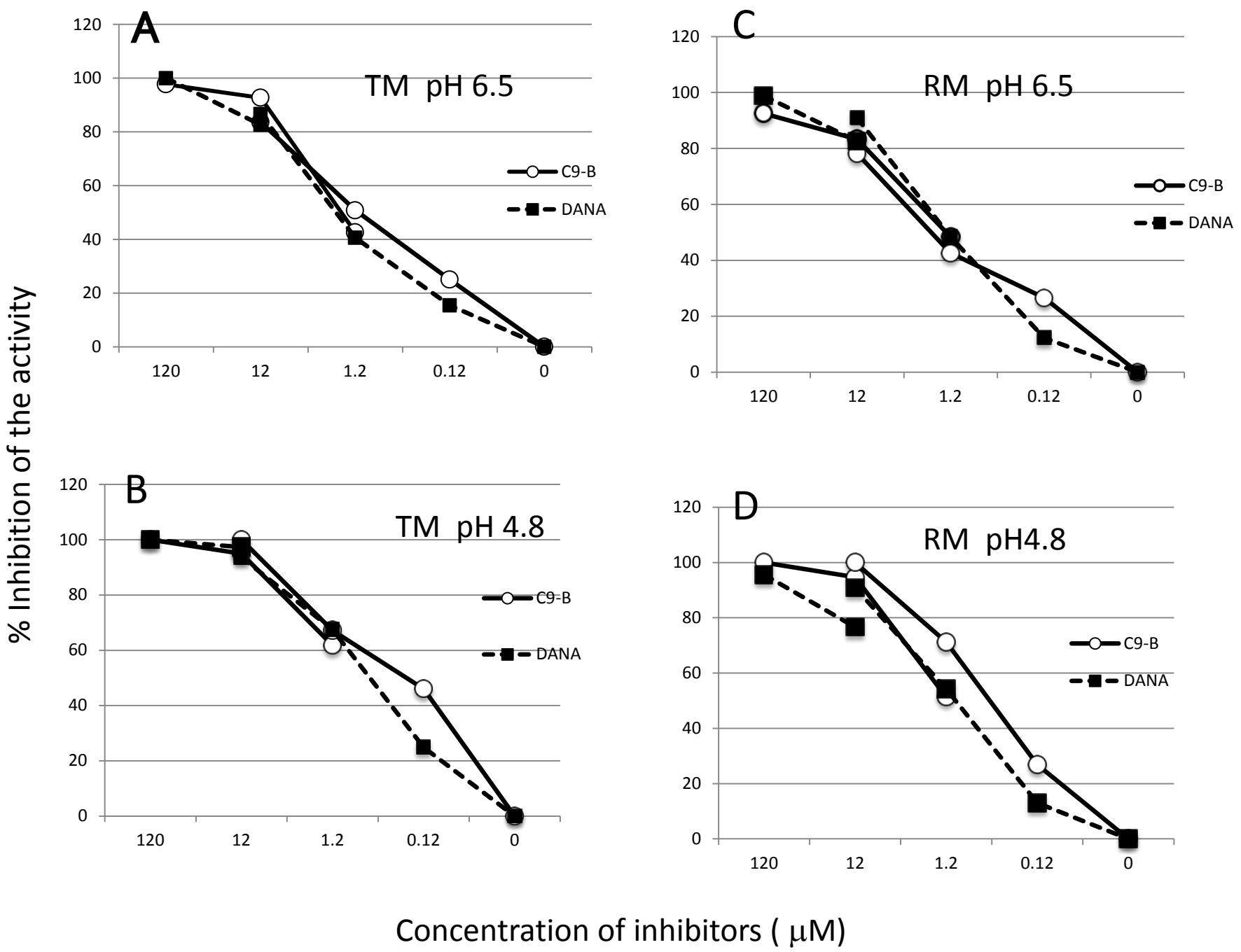
A
TM pH 6.5
C9-B
DANA
120
100
80
60
40
20
0
120
12
1.2
0.12
0
B
TM pH 4.8
C
RM pH 6.5
D
RM pH4.8
% Inhibition of the activity
Concentration of inhibitors (μM)

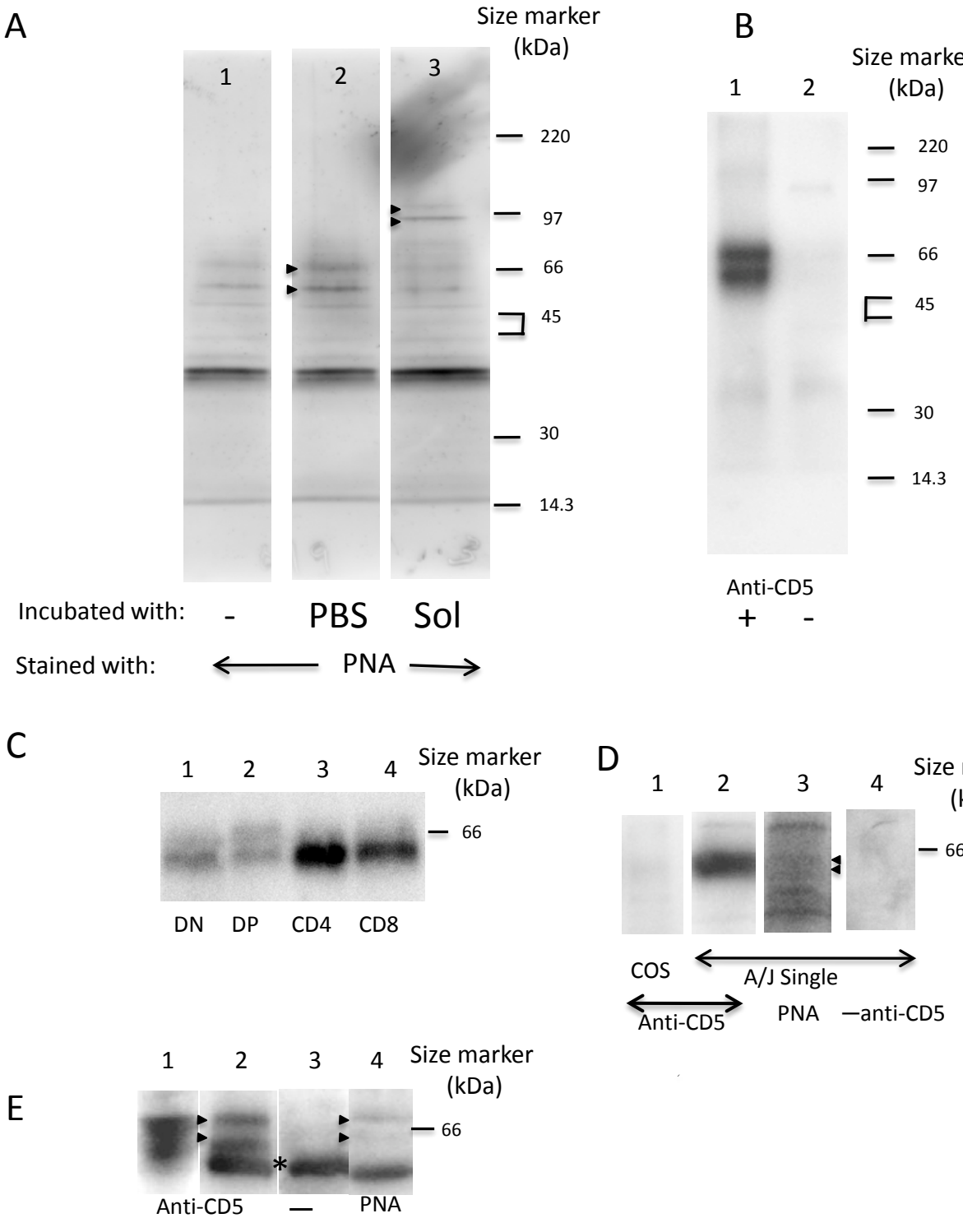
A
Size marker (kDa)
1
2
3
220
97
66
45
30
14.3
Incubated with: - PBS Sol
Stained with: PNA
B
Size marker (kDa)
1
2
220
97
66
45
30
14.3
Anti-CD5
+ -
C
1
2
3
4
Size marker (kDa)
66
DN DP CD4 CD8
D
1
2
3
4
Size marker (kDa)
66
COS
A/J Single
Anti-CD5
PNA —anti-CD5
E
1
2
3
4
Size marker (kDa)
66
*
Anti-CD5 —
PNA

Supplementary Table

Position	Score
96 (S)	0.690318
138 (T)	0.931411
139 (T)	0.953766
143 (T)	0.967977
144 (T)	0.969745
145 (T)	0.950114
148 (T)	0.961988
149 (T)	0.852004
154 (T)	0.88879
221 (T)	0.856794
365 (T)	0.571536
475 (T)	0.706253

Table Legend: Scores obtained from NetOGlyc 4.0 on the murine CD5 amino acid sequence as reported in UniProt, indicating eight possible O-glycosylation sites (138T~154T) with high probability.